Journal of Alloys and Compounds 500 (2010) 175–180

Contents lists available at ScienceDirect

Journal of Alloys and Compounds

journal homepage: www.elsevier.com/locate/jallcom

Preparation and annealing of GaN/Cu core-shell nanowires

Hyoun Woo Kim*, Hyo Sung Kim, Han Gil Na, Ju Chan Yang, Chongmu Lee

Division of Materials Science and Engineering, Inha University, Incheon 402-751, Republic of Korea

ARTICLE INFO

Article history:
Received 22 December 2009
Received in revised form 24 March 2010
Accepted 31 March 2010
Available online 8 April 2010

Keywords:
GaN
Nanowires
Cu
Plasma sputtering
Thermal annealing

ABSTRACT

GaN-core/Cu-shell nanowires were prepared and their annealing behavior was investigated. The thermal annealing induced the surface-roughening of the hetero-nanowires due to the agglomeration and generation of cluster-like structures from the Cu-shell layers. X-ray diffraction suggested that the thermal annealing generated CuO_x phases. The core GaN nanowires exhibited weak ferromagnetism at 5 K and their coercivity was increased by Cu-sputtering and subsequent thermal annealing at 800 °C. In the Gaussian deconvolution studies, the photoluminescence (PL) spectra exhibited emission bands centered at 2.0 and 3.2 eV, irrespective of the Cu-coating and/or thermal annealing. A mechanism is proposed to explain the significant change in the intensity of the ultraviolet (UV) emission by the combination of Cu-sputtering and annealing at 1000 °C.

1. Introduction

Nanowires have attracted considerable attention due to their specific physical and chemical properties and their potential applicability to a variety of nanoscale devices and systems [1–7]. Due to its unique properties that include a large direct bandgap, strong interatomic bonds, and high thermal conductivity [8], gallium nitride (GaN) can be used in the formulation of light-emitting and optoelectronic devices [9,10]. Thus, the synthesis of GaN nanowires has been intensively studied [11–14]. On the other hand, copper (Cu) nanowires display many useful physical properties; they are particularly suitable for applications in nanodevices owing to their low electrical resistivity and low cost [15]. For example, Cu has been widely used as ultra-large-scale integration (ULSI) interconnects to reduce the resistance–capacitance delay, the amount of electromigration, and the cost of fabrication [16]. Cu doping has been studied for a variety of applications, including Cu-doped ZnO nanowires for photodetectors [17] and ferromagnetism [18,19].

In order to enhance the functionality of nanowires and protect them against contamination, radial heterostructured nanowires have been created [20–22]. For example, in optoelectronic applications, by selecting lattice-misfitting core-shell combinations, the emission efficiency can be enhanced, while the band gap can be tailored through strain effects and quantum confinement [23]. For lithium ion battery applications, the core nanowires function as electron transport pathways and as a type of stable mechanical support, whereas the shell layers, with sufficient mechanical strength, act as a structural buffer [24]. Moreover, a new surface plasmon resonance band has been generated from the bimetallic interface of metallic core-shell nanowires [25]. Also, metallic core-shell nanowires showed enhanced magnetic properties in comparison to those of pure core metal nanowires [26]. The photoluminescence stability of the core nanowires is enhanced by the shell coating [27] and the new emission was generated from the structural defects originating from the heterostructure interface [22]. The presence of dielectric shells around the semiconductor core nanowires enables the realization of surround-gate nanowire field-effect transistors [28]. In this study, core GaN nanowires were coated with Cu-shell layers using a plasma sputtering method. In next-generation devices, Cu metallization will be a predominant technology. Although it is anticipated that a thin diffusion layer will be inserted between GaN and Cu in practical devices, a GaN/Cu scheme without such a barrier deserves a thorough investigation. A Cu–Ag ohmic contact on p-type GaN has also been investigated [29]. In particular, as the fabrication of ULSIs inevitably involves a high-temperature process, it is crucial to investigate the thermal heating effects. Accordingly, the thermal annealing of hetero-nanowires was carried out. In this case, some physical and chemical changes are to be expected, possibly including the diffusion of Cu into the GaN lattice. In a previous investigation involving Cu-implanted GaN films [30], Cu dopant was intrinsically nonmagnetic in its natural state. Understanding the mechanism of ferromagnetism in a nonmagnetic element doped semiconductor is useful in exploring new areas of dilute magnetic semiconductors. Additionally, Cu implantation into GaN films can induce intrinsic defects, significantly changing the optical and magnetic properties [30–32]. Herein, the fabrication of GaN/Cu core-shell nanowires is initially reported and the structural, photoluminescence (PL), and magnetic

* Corresponding author. Tel.: +82 32 860 7544; fax: +82 32 862 5546.
E-mail address: hwkim@inha.ac.kr (H.W. Kim).

0925-8388/$ – see front matter © 2010 Elsevier B.V. All rights reserved.
doi:10.1016/j.jallcom.2010.03.234

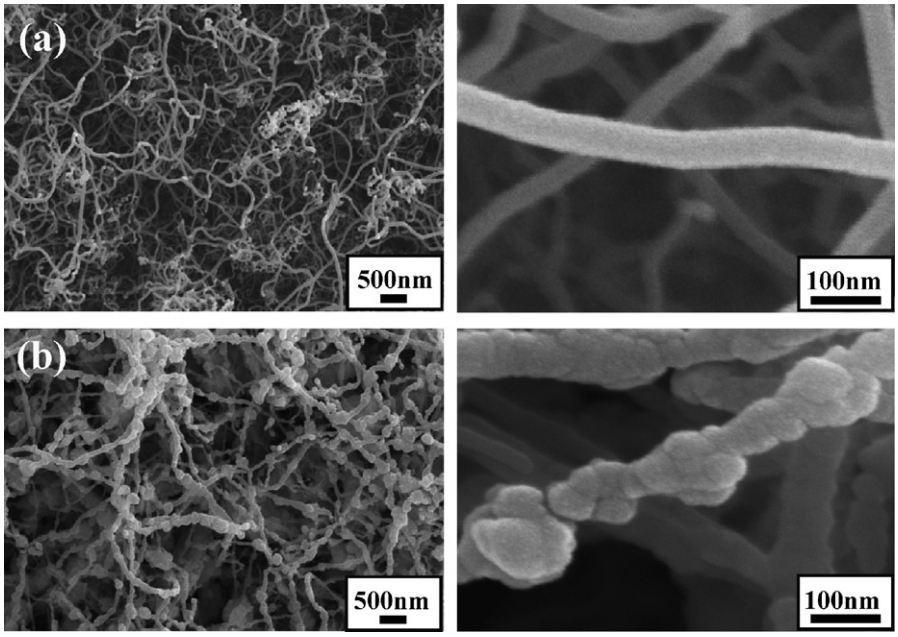

Fig. 1. SEM images of the core/shell nanowires (a) before and (b) after thermal annealing at 800 °C.

properties of the as-synthesized GaN/Cu core-shell nanowires are investigated.

2. Experimental

Core GaN nanowires were fabricated on silver (Ag: about 10 nm)-coated Si substrates by heating pure GaN powders. The flow rates of Ar and NH_3 were 100 and 20 sccm, respectively. The reaction temperature was 1000 °C and the growth was conducted for 1 h. A similar synthetic strategy was adopted in a previous experiment conducted by the authors, in which MgO nanowires [33] and SnO_2 nanowires [34] were fabricated. Subsequently, the substrates were sputtered in a turbo sputter coater with the Cu target installed (Emitech K575X, Emitech Ltd., Ashford, Kent, UK) [35]. At room temperature, the sputter time was set to 90 s under flowing argon (Ar) gas with a DC sputtering current of 65 mA. Subsequently, the as-fabricated samples were annealed for 30 min at 400–800 °C in air ambient under flowing Ar.

The samples were analyzed by powder X-ray diffraction (XRD, Philips X'pert MRD diffractometer), scanning electron microscopy (SEM, Hitachi, S-4200), transmission electron microscopy (TEM, Philips CM-200), selected area electron diffraction (SAED), and energy dispersive X-ray spectroscopy (EDX). Room-temperature photoluminescence (PL) measurements were carried out to study the optical properties of the core-shell nanowires using a He–Cd laser with a wavelength of 325-nm line as the excitation source at a power level of 55 mW. The magnetic properties of the samples were investigated using the superconducting quantum interference device (SQUID) magnetometers (Quantum Design MPMS-7 for hysteresis measurement) at KBSI.

3. Results and discussion

Fig. 1a and b shows the SEM images of the GaN-core/Cu-shell nanowires in the as-fabricated state and after annealing at 800 °C, respectively. Although both products consist of one-dimensional (1D) structures, the SEM images on the right clearly show that the nanowire surface was considerably changed by the thermal annealing. The surface became noticeably rougher after annealing, suggesting that morphological changes occurred in the shell layer.

Fig. 2a shows an XRD pattern of the as-fabricated GaN-core/Cu-shell nanowires, in which the entire spectrum can be indexed to the crystalline hexagonal wurtzite GaN phase (JCPDS card: No. 02-1078). Fig. 2b shows the XRD spectrum of the GaN nanowires that were Cu-sputtered and annealed at 400 °C. Apart from the diffraction peaks of the hexagonal wurtzite GaN phase (JCPDS card: No. 02-1078), there exists a (2 0 0) peak of the cubic Cu_2O phase with a lattice constant of $a = 0.4267$ nm (JCPDS card: No. 78-2076). Fig. 2c shows the XRD spectrum of the GaN nanowires that were Cu-

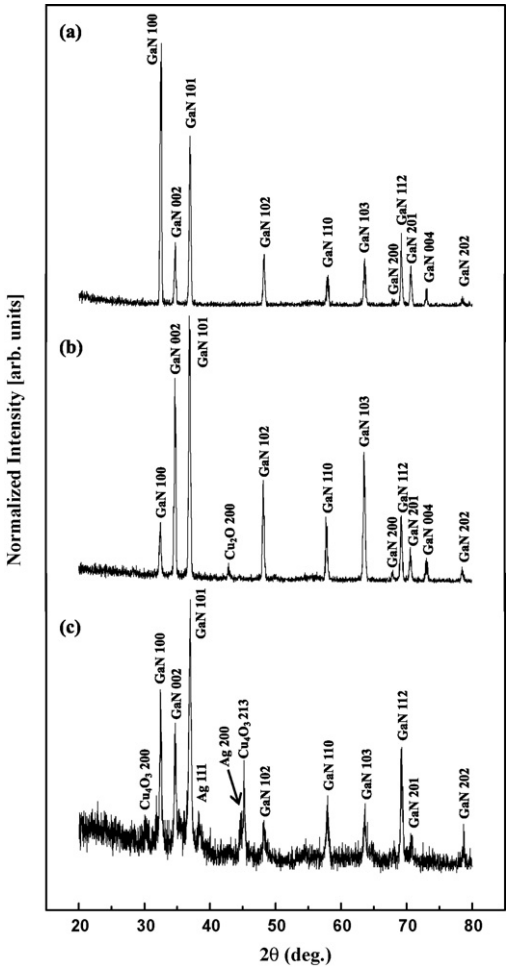

Fig. 2. XRD patterns of (a) as-synthesized GaN-core/Cu-shell nanowires, (b) GaN nanowires which were Cu-sputtered and annealed at 400 °C, and (c) GaN nanowires which were Cu-sputtered and annealed at 800 °C.

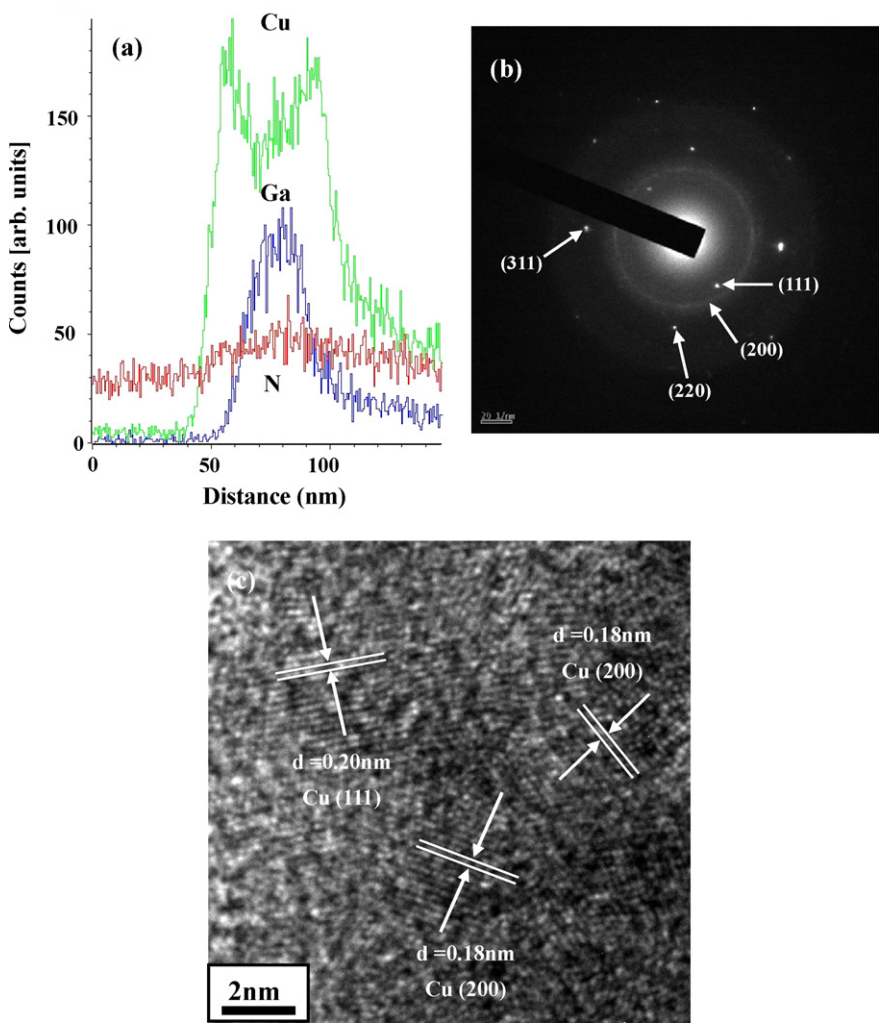

Fig. 3. (a) TEM-EDX line concentration profiles for Ga, N, and Cu along a line drawn across the diameter of an as-fabricated GaN–Cu core-shell nanowire. (b) Corresponding SAED pattern. (c) Lattice-resolved TEM image enlarging an area near the surface of the nanowire.

sputtered and annealed at 800 °C. The figure shows the (2 0 0) and (2 1 3) peaks of a body-centered tetragonal Cu_4O_3 phase with lattice constants of $a = 0.583$ nm and $c = 0.988$ nm (JCPDS card: No. 03-0879).

Accordingly, the Cu_2O phase was most likely generated by the thermal annealing at 400 °C. In addition, the Cu_2O phase can be oxidized further to the Cu_4O_3 phase by thermal annealing at a higher temperature of 800 °C. Although a previous report revealed that varying the oxygen partial pressure during the dc magnetron sputtering process led to the synthesis of different copper oxides such as Cu_2O, Cu_4O_3, and CuO [36], there have been no reports on the temperature-dependent variation of the phases. Further detailed studies will therefore be needed. On the other hand, it is noteworthy that weak reflection peaks exist corresponding to the cubic Ag phase (JCPDS card: No. 04-0783), presumably originating from the Ag layer predeposited on the Si substrate. Hence, the Ag at the bottom likely played a catalytic role in the growth of the GaN nanowires. The Ga-related vapor that is generated combines with Ag on the substrate, and the supersaturation of the liquid alloy droplets brings about the precipitation of short GaN nuclei from which GaN nanowires subsequently grow.

Fig. 3a shows the concentration profiles for Ga, N, and Cu along a line drawn across the diameter of a GaN–Cu core-shell nanowire. Ga element is mainly encountered in the core of the coaxial nanowires, whereas Cu is mainly located in the shell region, which has a valley-like profile. Fig. 3b shows an associated SAED pattern, exhibiting the diffraction rings of cubic Cu (JCPDS card: No. 04-0836). Fig. 3c shows an enlarged lattice-resolved TEM image of a crystalline region, revealing that the spacings between the lattice planes are approximately 0.20 and 0.18 nm, corresponding to d_{111} and d_{200} of cubic Cu, respectively.

Fig. 4a shows a low-magnification TEM image of a GaN nanowire which was Cu-sputtered and annealed at 800 °C, exhibiting blackened cluster-like regions. Fig. 4b and c shows the associated EDX elemental maps of Ga and Cu, respectively. Accordingly, the cluster-like structures indicated by the arrowheads in Fig. 4a are comprised of Cu elements. Fig. 4d shows the associated SAED pattern, confirming the existence of the cubic Cu_4O_3 phase. Fig. 4e is a lattice-resolved TEM image, revealing that the spacings between the lattice planes are nearly 0.31, 0.29, and 0.25 nm, corresponding to the d_{112}, d_{200}, and d_{202} spacings of cubic Cu_4O_3, respectively.

Fig. 5a shows the magnetic hysteresis loop of the core GaN nanowires and Fig. 5b shows that of the GaN nanowires which were Cu-sputtered and annealed at 800 °C. At 5 K, clear hysteresis loops are observed in both samples; these were corrected for the diamagnetic component arising from the substrates. The core GaN nanowires in the present study exhibited weak ferromagnetism at 5 K. It is known that the ferromagnetism of undoped GaN originates mainly from Ga vacancies [37,38].

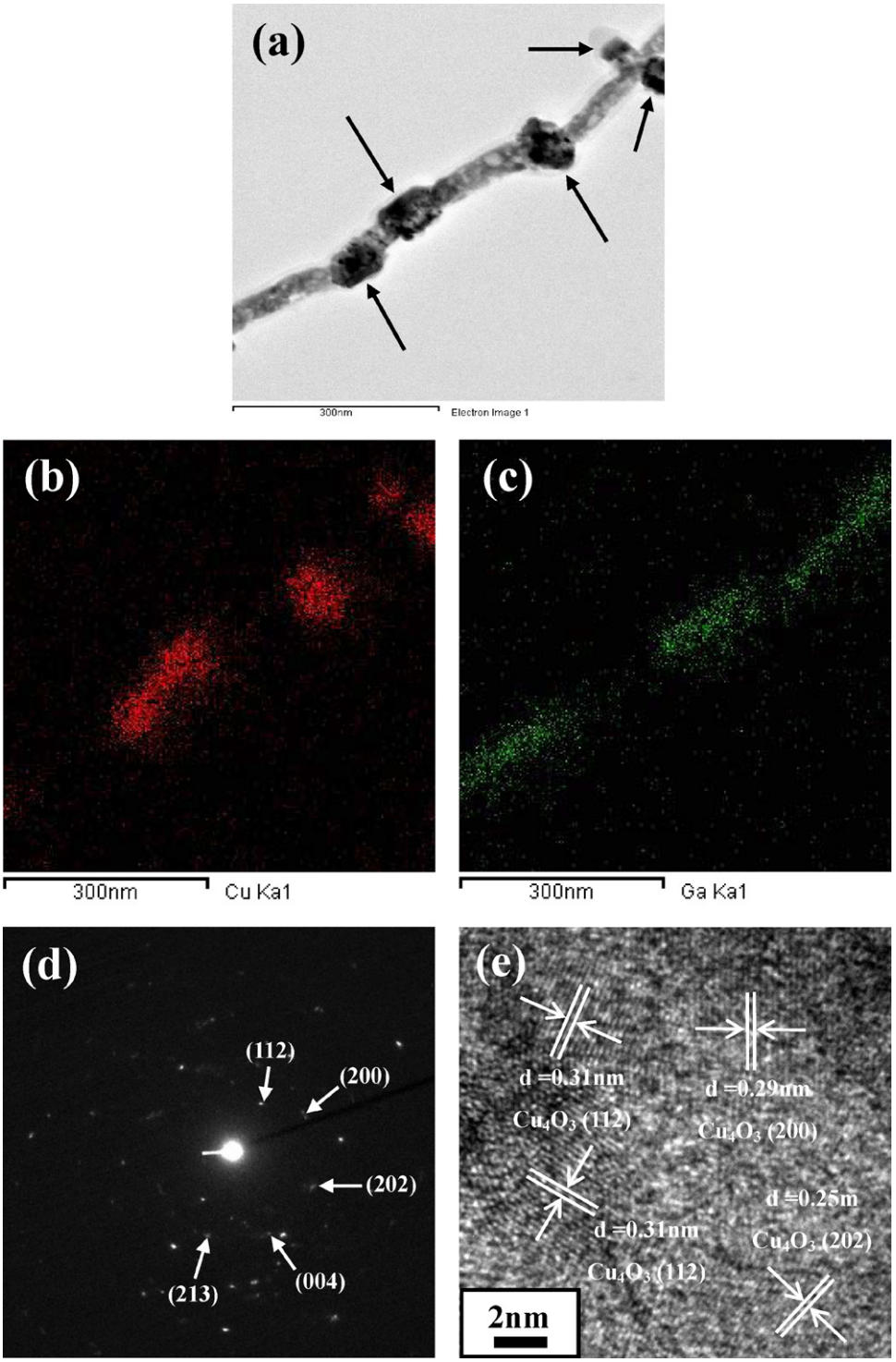

Fig. 4. (a) TEM image of a GaN nanowire which was Cu-sputtered and annealed at 800 °C. TEM-EDX elemental maps of (b) Cu and (c) Ga concentrations from a Cu-coated nanowire after thermal annealing at 800 °C. (d) Corresponding SAED pattern. (e) Lattice-resolved TEM image enlarging an area near the surface of the nanowire.

From the lower-right insets, which are magnified sections of the curve around the zero magnetic field, the coercivity and squareness were estimated. The squareness (remanent magnetization/saturated magnetization) of the core nanowires and GaN nanowires, which were Cu-sputtered and annealed at 800 °C, were estimated to be approximately 0.1, revealing that the squareness was not changed by the Cu-coating and subsequent thermal annealing. However, the coercivities of the core nanowires and the samples annealed at 800 °C were found to be 139 Oe (1 Oe = 79.57747 Am^{-1}) and 652 Oe, respectively. It is clear that the coercivity was increased by the Cu-sputtering and subsequent thermal annealing at 800 °C. Accordingly, the negative applied field necessary for achieving the zero magnetization of the Cu-sputtered GaN nanowires annealed at 800 °C was greater than that of the core GaN nanowires.

Wu et al. proposed that the ferromagnetism in Cu-doped GaN can be attributed to the indirect ferromagnetic coupling among the dopants, which is referred to as p–d hybridization [39]. In the

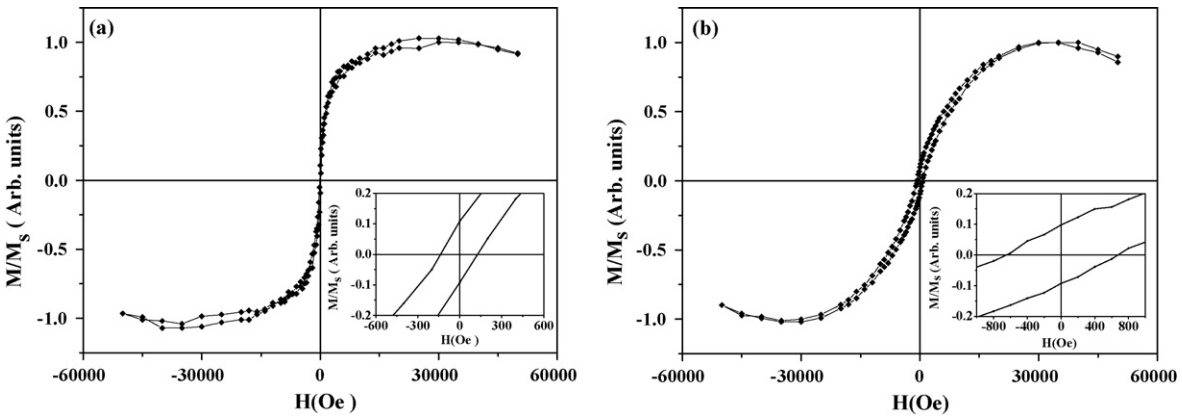

Fig. 5. Hysteresis loops for (a) core GaN nanowires and (b) GaN nanowires which were Cu-sputtered and annealed at 800 °C (Ms: saturated magnetization; M: magnetization). The inset shows a magnified section of the curve around the zero magnetic field.

present case, although XRD revealed that a considerable number of Cu atoms are consumed to generate the Cu_4O_3 phase during thermal annealing at 800 °C, it is possible that Cu dopants reside in the GaN lattice at a low concentration. In addition, it has been proposed that the defects, including gallium vacancies (V_{Ga}) and defect complexes (e.g., Cu_{Ga}–V_N or V_{Ga}–O_N), play an important role in the ferromagnetism in Cu-doped GaN [30,40]. In another study, Rosa et al. demonstrated that the weak ferromagnetism of Cu-doped GaN can be ascribed to nitrogen vacancies (V_N) [40]. Accordingly, the origin of the observed ferromagnetic order in the Cu-shelled GaN nanowires can be explained not only by the Cu dopants, but also by the vacancy-related defects. Although the mechanism by which Cu affects the formation of these defects is unknown, the subsequent thermal annealing process activates the Cu diffusion in the GaN lattice and/or increases the generation of vacancies, thereby enhancing the ferromagnetic behavior. The other possibility is that the ferromagnetism is enhanced by vacancies in the Cu_4O_3 phase. Although Cu_4O_3 [41] normally does not exhibit ferromagnetic behavior, it is possible that the ferromagnetism originates from oxygen and copper vacancies [42].

PL measurements were carried out for the core GaN nanowires, the as-fabricated GaN/Cu core-shell nanowires, and the Cu-coated

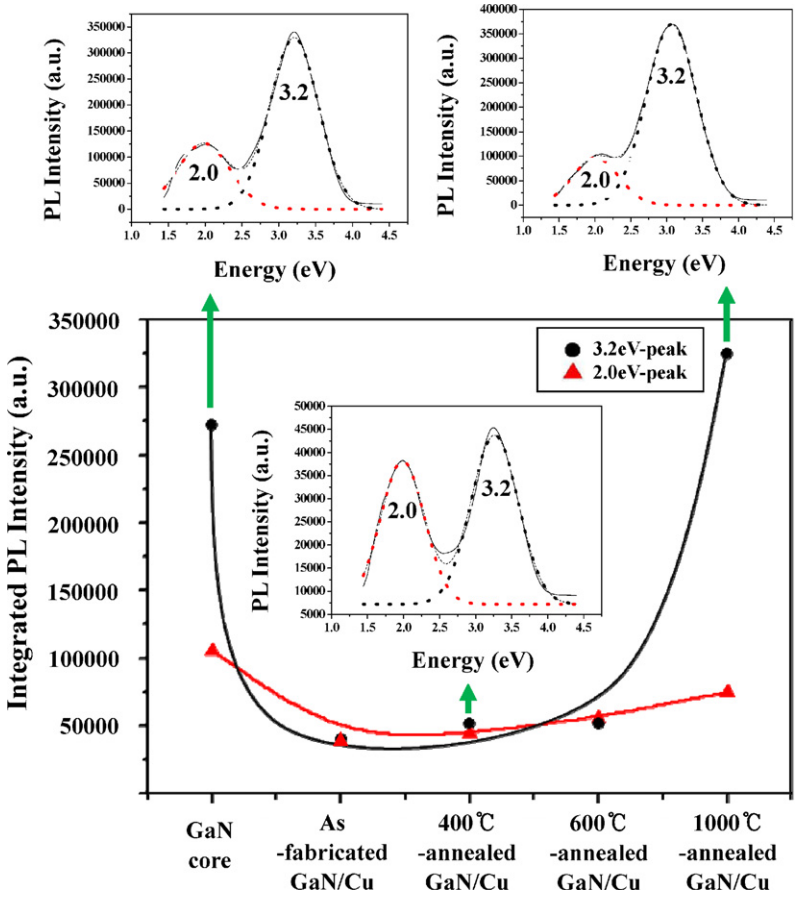

Fig. 6. Integrated PL intensities of uncoated core GaN nanowires, Cu-coated GaN nanowires prior to thermal annealing, and Cu-coated GaN nanowires after thermal annealing at 400, 600, and 1000 °C.

nanowires annealed at 400, 600, and 1000 °C (Fig. 6). All of the emission spectra can be deconvoluted into two broad bands, the first centered at 3.2 eV in the ultraviolet (UV) region and the second at 2.0 eV in the red region. The red emission band in GaN is generally attributed to the vacancy-impurity pairs, including $V_{Ga}Si$, V_NMg, V_NC_N, and $V_{Ga}O_N$ [43–47]. On the other hand, the UV band in GaN is attributed to the transition from a shallow donor to a shallow acceptor [48]. The main candidates for the shallow donors are Si_{Ga} and O_N, whereas those for the shallow acceptors are Si_N and C_N [48]. As a dopant was not intentionally introduced in this synthesis environment, the origin of the red and UV emissions is related to the diffusion of Si from the substrate and C and O from inside the chamber; these are activated by thermal evaporation at a sufficiently high temperature of 1000 °C.

In the Cu-coated GaN nanowires, subsequent thermal annealing in the range of 400–600 °C slightly increases the intensity of both the red and UV emissions, presumably because it not only contributes to the generation of native defects (including vacancies) but also enhances the introduction/diffusion of emission-related impurities. Moreover, it was observed that the intensities of the red and UV emissions are slightly but significantly reduced by Cu-sputtering. For both emissions, the reduced intensity was restored by thermal annealing at a sufficiently high temperature.

The UV–vis absorption spectrum of the Cu nanoparticles indicates that the Cu absorbs a significant amount of UV light, with relatively weak absorption in the visible region [49]. Accordingly, it is likely that the PL emission from the GaN-core nanowires can be absorbed in the Cu-shell layer, resulting in a significantly reduced UV emission. In addition, the Cu-shell layer can absorb some of the excitation light at 325 nm, as well as the PL emission from the GaN-core. However, no reduction in intensity is observed in the samples which underwent thermal annealing at a sufficiently high temperature, presumably because a considerable part of the GaN-core is exposed by the thermal agglomeration of the Cu-shell layer (as shown in Fig. 4). Although the absorption in Cu will be followed by the relaxation of the excited electron and subsequent fluorescent emission [49], the relative intensity of the emission/excitation is less than unity. Although further study is in progress in an attempt to reveal the detailed mechanism of the intensity variation, it is tentatively suggested here that the Cu-shell layer plays a role in the abrupt reduction of the UV emission.

4. Conclusions

In summary, GaN-core/Cu-shell nanowires were fabricated and the effects of the subsequent thermal annealing process were investigated. The XRD investigation revealed that thermal annealing at 800 °C generated the Cu_4O_3 phase. The TEM elemental maps indicated that thermal annealing facilitates the generation of cluster-like structures which are comprised of Cu elements. The core GaN nanowires exhibited weak ferromagnetism at 5 K and their coercivity was increased by Cu-sputtering and subsequent thermal annealing at 800 °C. The PL spectra of the GaN/Cu core-shell nanowires were deconvoluted into two broad bands, the first centered at 3.2 eV in the UV region and the second at 2.0 eV in the red region. The integrated intensity of the UV emission of the core GaN nanowires was significantly reduced by Cu-coating, whereas it was restored by thermal annealing at a sufficiently high temperature. Hence, the associated mechanism is most likely related to the absorption by the Cu-shell layers.

Acknowledgements

This research was funded by the Small & Medium Business Administration, Ministry of Knowledge Economy (S1025549).

References

[1] Y.N. Xia, P.D. Yang, Y.G. Sun, Y.Y. Wu, B. Mayers, B. Gates, Y.D. Yin, F. Kim, Y.Q. Yan, Adv. Mater. 15 (2003) 353.
[2] R.E. Algra, M.A. Verheijen, M.T. Borgström, L. Feiner, G. Immink, W.J.P. van Enckevort, E. Vlieg, E.P.A.M. Bakkers, Nature 456 (2008) 369.
[3] A.I. Boukai, Y. Bunimovich, J. Tahir-Kheli, J.-K. Yu, W.A. Goddard III, J.R. Heath, Nature 451 (2008) 168.
[4] V.V. Deshpande, M. Bockrath, L.I. Glazman, A. Yacoby, Nature 464 (2010) 209.
[5] C.-Y. Wen, M.C. Reuter, J. Bruley, J. Tersoff, S. Kodambaka, E.A. Stach, F.M. Ross, Science 326 (2009) 1247.
[6] Y. Shen, T. Yamazaki, Z. Liu, D. Meng, T. Kikuta, J. Alloys Compd. 488 (2009) L21.
[7] H. Liu, D. Wexler, G. Wang, J. Alloys Compd. 487 (2009) L24.
[8] J. Neugebauer, C.G. Van de Walle, Appl. Phys. Lett. 69 (1996) 503.
[9] B. Liu, Y. Bando, C. Tang, F. Xu, J. Hu, D. Golberg, J. Phys. Chem. B 109 (2005) 17082.
[10] H.Q. Jia, L.W. Guo, W.X. Wang, H. Chen, Adv. Mater. 45 (2009) 4641.
[11] Y. Huang, X. Duan, Y. Cui, C.M. Lieber, Nano Lett. 2 (2002) 101.
[12] H.M. Kim, Y.H. Choo, H. Lee, S.I. Kim, S.R. Ryu, D.Y. Kim, T.W. Kang, K.S. Chung, Nano Lett. 4 (2004) 1059.
[13] J. Chen, C. Xue, H. Zhuang, Z. Yang, L. Qin, H. Li, Y. Huang, J. Alloys Compd. 468 (2009) L1.
[14] P.G. Li, X. Guo, X. Wang, W.H. Tang, J. Alloys Compd. 475 (2009) 463.
[15] W.F. Zhou, G.T. Fei, X.F. Li, S.H. Xu, L. Chen, B. Wu, L.D. Zhang, J. Phys. Chem. C 113 (2009) 9568.
[16] Q. Huang, C.M. Lilley, R. Divan, Nanotechnology 20 (2009) 075706.
[17] N. Kouklin, Adv. Mater. 20 (2008) 2190.
[18] M. Shuai, L. Liao, H.B. Lu, J. Phys. D-Appl. Phys. 41 (2008) 135010.
[19] D.Q. Gao, Y. Xu, Z.H. Zhang, H. Gao, D.S. Xue, J. Appl. Phys. 105 (2009) 063903.
[20] L.J. Lauhon, M.S. Gudiksen, C.L. Wang, C.M. Lieber, Nature 420 (2002) 57.
[21] T.J. Morrow, M. Li, J. Kim, T.S. Mayer, C.D. Keating, Science 323 (2009) 352.
[22] M. Lei, L.Q. Qian, Q.R. Hu, S.L. Wang, W.H. Tang, J. Alloys Compd. 487 (2009) 568.
[23] I.A. Goldthorpe, A.F. Marshall, P.C. McIntyre, Nano Lett. 9 (2009) 3715.
[24] J. Liu, Y. Li, R. Ding, J. Jiang, Y. Hu, X. Ji, Q. Chi, Z. Zhu, X. Huang, J. Phys. Chem. B 113 (2009) 5336.
[25] J. Zhu, Nanoscale Res. Lett. 4 (2009) 977.
[26] S.-C. Lin, S.-Y. Chen, Y.-T. Chen, S.-Y. Cheng, J. Alloys Compd. 449 (2008) 232.
[27] C.-C. Wang, C.-C. Kei, Y. Tao, Y.-P. Perng, Electrochem. Sol. Stat. Lett. 12 (2009) K49.
[28] E. Sutter, F. Camino, P. Sutter, Appl. Phys. Lett. 94 (2009) 083109.
[29] J.H. Son, G.H. Jung, J.-L. Lee, Appl. Phys. Lett. 93 (2008) 012102.
[30] X.L. Yang, Z.T. Chen, C.D. Wang, Y. Zhang, X.D. Pei, Z.J. Yang, G.Y. Zhang, Z.B. Ding, K. Wang, S.D. Yao, J. Appl. Phys. 105 (2009) 053910.
[31] L. Sun, F. Yan, H. Zhang, J. Wang, Y. Zeng, G. Wang, J. Li, Appl. Surf. Sci. 256 (2009) 1631.
[32] B. Zhang, C.C. Chen, C. Yang, J.Z. Wang, L.Q. Shi, H.S. Cheng, D.G. Zhao, Nucl. Instr. Meth. B 268 (2010) 123.
[33] H.W. Kim, S.H. Shim, Chem. Phys. Lett. 422 (2006) 165.
[34] H.W. Kim, J.W. Lee, S.H. Shim, C. Lee, J. Korean Phys. Soc. 51 (2007) 198.
[35] H.W. Kim, S.H. Shim, J.W. Lee, Carbon 45 (2007) 2695.
[36] H. Zhu, J. Zhang, C. Li, F. Pan, T. Wang, B. Huang, Thin Solid Films 517 (2009) 5700.
[37] H. Jin, Y. Dai, B.B. Huang, M.-H. Whangbo, Appl. Phys. Lett. 94 (2009) 162505.
[38] P. Dev, Y. Xue, P. Zhang, Phys. Rev. Lett. 100 (2008) 117204.
[39] R.Q. Wu, G.W. Peng, L. Liu, Y.P. Feng, Z.G. Huang, Q.Y. Wu, Appl. Phys. Lett. 89 (2006) 062505.
[40] A.L. Rosa, R. Ahuja, Appl. Phys. Lett. 91 (2007) 232109.
[41] M.-H. Whangbo, H.-J. Koo, Inorg. Chem. 41 (2002) 3570.
[42] C. Chen, L. He, L. Lai, H. Zhang, J. Lu, L. Guo, Y. Li, J. Phys.: Condens. Matter 21 (2009) 145601.
[43] S. Nakamura, N. Iwasa, M. Senoh, T. Mukai, Jpn. J. Appl. Phys. 31 (1992) 1258.
[44] U. Kaufmann, M. Kunzer, H. Obloh, M. Maier, Ch. Manz, A. Ramakrishnan, B. Santic, Phys. Rev. B 59 (1999) 5561.
[45] D.M. Hofmann, B.K. Meyer, H. Alves, F. Leiter, W. Burkhard, N. Romanov, Y. Kim, J. Krüger, E.R. Weber, Phys. Stat. Sol. (a) 180 (2000) 261.
[46] L. Wang, E. Richter, M. Weyers, Phys. Stat. Sol. (a) 204 (2007) 846.
[47] S. Zeng, G.N. Aliev, D. Wolverson, J.J. Davies, S.J. Bingham, D.A. Abdulmalik, P.G. Coleman, T. Wang, P.J. Parbrook, Phys. Stat. Sol. (c) 3 (2006) 1919.
[48] M.A. Reshchikov, H. Morkoc, J. Appl. Phys. 97 (2005) 061301.
[49] O.P. Siwach, P. Sen, J. Nanopart. Res. 10 (2008) 107.